

Driven Ratchets with Disordered Tracks

Thomas Harms and Reinhard Lipowsky

MPI für Kolloid- and Grenzflächenforschung, Kantstrasse 55, D-14513 Teltow-Seehof, Germany

(Received 20 December 1996)

The stochastic motion of ratchets is studied in the context of driven or pumped two-state models. For completely ordered tracks, the ratchets can be characterized both by an effective drift velocity and an effective diffusion coefficient on large scales. These properties are strongly perturbed by the presence of frozen disorder or defects along the tracks. Depending on the defect concentration and on the transition rates between the two states, the ratchets now exhibit several scaling regimes with anomalous transport properties. [S0031-9007(97)04225-7]

PACS numbers: 05.40.+j, 05.70.Ln, 87.10.+e

Ratchets are model systems for nonequilibrium transport based on the rectification of thermal fluctuations. This rectification can arise from chemical reactions as envisaged in the classical work on muscle contraction [1] or if different parts of the ratchet are at different (effective) temperatures [2]. Recently, new experimental results on motor proteins [3] have stimulated a lot of theoretical work on such ratchets [4–9]. In addition, ratchets have also been discussed theoretically as models for intracellular energy transduction via protrusive forces [10], and artificial ratchets have been constructed experimentally using microstructured electrodes [11] and optical tweezers [12].

Most of this work was concerned with single-particle ratchets. Such a ratchet has the following basic features: (i) It consists of a “particle” which can move along a one-dimensional “track” where it is subject to a spatially asymmetric potential. The average potential is flat, however, and there is no average force acting on the particle. (ii) The particle can overcome the barriers of the potential via thermally excited fluctuations. (iii) The particle also feels a time-dependent external driving force or pumping mechanism which acts to rectify these thermal fluctuations.

In all previous work on single-particle ratchets, the asymmetric potential was taken to be periodic in space corresponding to a completely ordered track. In contrast, we will consider tracks which contain a certain amount of frozen *disorder* or *defects* and study the effects of this disorder on the transport properties of the ratchet. In order to illustrate our results, we will explicitly discuss ratchets with sawtooth potentials for which the defects correspond to reversed sawteeth as shown in Fig. 1.

It will be shown below that defects act to reduce the efficiency of the ratchets and that this efficiency loss has two general and nontrivial features: (i) The motion of the ratchets is most sensitive to the frozen disorder if it operates in the “resonance regime,” i.e., in the regime where it is most effective in the absence of disorder, and (ii) depending on the defect concentration, the ratchets exhibit several scaling regimes with anomalous diffusion and/or anomalous drift. These regimes should be accessible to experiments on natural or artificial ratchets.

To proceed, we will consider a particle which moves along a one-dimensional track with coordinate x and which has two internal states, its ground state 1 and its excited state 2. It is coupled to another energy producing process (such as a chemical reaction) which induces transitions from its ground state to its excited state with frequency ω_1 and transitions back to its ground state with frequency ω_1 . Depending on its internal state, the particle is subject to two different external potentials $U_1(x)$ and $U_2(x)$ which have a microscopic range denoted by a . The particle motion is overdamped with frictional coefficient f in both states, and its surroundings have the ambient temperature T (measured in energy units, i.e., the Boltzmann factor has been absorbed into the symbol T).

The basic dynamical quantities for this stochastic system are the distribution functions $P_1(x, t)$ and $P_2(x, t)$ which describe the probabilities at time t that the particle has reached the location x and is in states 1 and 2, respectively. These quantities are governed by a generalized Fokker-Planck equation which we write in the compact form

$$\frac{\partial}{\partial t} \mathbf{P} = [\hat{F} + \hat{\Omega}] \mathbf{P}, \quad \text{with } \mathbf{P} \equiv \begin{pmatrix} P_1 \\ P_2 \end{pmatrix}. \quad (1)$$

The Fokker-Planck operator \hat{F} is diagonal with [13] $\hat{F}_{\alpha\alpha} \equiv (1/f)(\partial/\partial x)(dU_\alpha/dx + T\partial/\partial x)$ for $\alpha = 1, 2$; the transition operator $\hat{\Omega}$ has the matrix elements $\hat{\Omega}_{11} = -\omega_1 = -\hat{\Omega}_{21}$ and $\hat{\Omega}_{12} = \omega_1 = -\hat{\Omega}_{22}$.

The basic length scale is given by the potential range a , the basic energy scale by the thermal energy T , and the basic time scale may be defined by $t_{sc} \equiv fa^2/T$. Thus, if length, energy, and time are measured in units of these

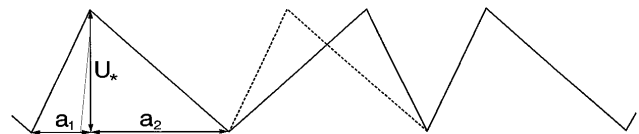


FIG. 1. Asymmetric sawtooth potential with one defect corresponding to a reversed sawtooth. Each sawtooth is characterized by its height U_* and the two length scales a_1 and a_2 with period $a = a_1 + a_2$.

basic scales, the behavior of the ratchet depends only (i) on the reduced potentials U/T and (ii) on the reduced transition rates ωt_{sc} .

For periodic potentials, i.e., in the absence of frozen disorder, the steady states of the above ratchet model have been previously studied in some detail [7,8]. In the steady state, one finds periodic distributions and a time-independent current. Now, we will first go *beyond* this steady state analysis and consider the motion of a particle which is initially described by a localized distribution. Numerical integration of the generalized Fokker-Planck equation (1) with periodic potentials shows that such a localized distribution evolves with time into a broad distribution which is modulated on the scale of the potential period a . After some initial transient behavior, the width of this distribution is large compared to a . In fact, one may introduce a coarse-grained probability distribution, denoted by \mathcal{P} , which behaves like a Gaussian wave packet with effective drift velocity v_0 and effective diffusion coefficient D_0 , and which thus satisfies the effective Fokker-Planck equation

$$\frac{\partial}{\partial t} \mathcal{P} = \frac{\partial}{\partial x} \left(-v_0 + D_0 \frac{\partial}{\partial x} \right) \mathcal{P}. \quad (2)$$

The two parameters v_0 and D_0 which enter in (2) can be determined from the following asymptotic expansion [14]. First, the probability $\mathbf{P} = (P_1, P_2)$ is expanded according to

$$\mathbf{P}(x, t) = \sum_{n=0}^{\infty} \mathbf{p}^{(n)}(x) \left(\frac{\partial}{\partial x} \right)^n \mathcal{P}(x/\lambda, t), \quad (3)$$

where the expansion parameter is given by a/λ . In zeroth order of this expansion, one finds that

$$[\hat{F} + \hat{\Omega}] \mathbf{p}^{(0)} = 0, \quad (4)$$

which, together with an appropriate normalization condition, determines $\mathbf{p}^{(0)} = (p_1^{(0)}, p_2^{(0)})$. The effective drift velocity is then given by

$$v_0 = -\frac{1}{f} \int_0^a dx \left\{ \frac{dU_1}{dx} p_1^{(0)}(x) + \frac{dU_2}{dx} p_2^{(0)}(x) \right\}. \quad (5)$$

This zeroth order result is equivalent to the results as obtained previously [7,8] from the steady state analysis.

In the next order of the expansion, the coefficient $\mathbf{p}^{(1)}$ which enters in (3) is determined from the inhomogeneous equation

$$[\hat{F} + \hat{\Omega}] p_{\alpha}^{(1)} = -\left(\frac{1}{f} \frac{dU_{\alpha}}{dx} + v_0 + 2 \frac{T}{f} \frac{\partial}{\partial x} \right) p_{\alpha}^{(0)} \quad (6)$$

with $\alpha = 1, 2$. Finally, one may calculate the effective diffusion coefficient via

$$D_0 = \frac{T}{f} \left(1 + \frac{a}{T} \int_0^a dx \times \left\{ \frac{dU_1}{dx} p_1^{(1)}(x) + \frac{dU_2}{dx} p_2^{(1)}(x) \right\} \right). \quad (7)$$

This iterative procedure may be applied, in general, to *any* two-state model as defined by (1) as long as the potentials and the transition rates are periodic in x . To be explicit, we will consider models for which U_1 is given by an asymmetric sawtooth potential, $U_2 \equiv 0$, and the transition rates do not depend on x .

In order to simplify the following discussion, the transition rates ω_{\uparrow} and ω_{\downarrow} are now taken to be identical and denoted by ω . In Fig. 2, we display the behavior of v_0 and D_0 for a sawtooth potential with $U_*/T = 10$ and $a_2/a_1 = 4$ as a function of the transition rate ω which varies over several orders of magnitude. In this figure, the solid lines and the circles represent the results of our iterative procedure and of the direct numerical integration of the Fokker-Planck equation (1), respectively; the broken lines correspond to the asymptotic behavior for small and for large ω as calculated analytically [15]. Inspection of Fig. 2 shows that the iterative procedure described above is very accurate for all values of ω .

The drift velocity v_0 exhibits a resonance regime close to its maximum at the intermediate frequency $\omega \equiv \omega_1$. When the particle is excited from its ground state in this regime, it spends just enough time in the excited state so that it can diffuse beyond the nearest potential barrier but not beyond the next-nearest one. The corresponding diffusion time $t_1 \simeq fa_1^2/T = (a_1/a)^2 t_{sc}$ which leads to the estimate $\omega_1 \simeq (a/a_1)^2 t_{sc}^{-1}$.

In order to introduce frozen disorder, it is convenient to consider a discrete mesh with lattice sites i and lattice constant a . The coarse-grained probability \mathcal{P}_i then satisfies

$$\begin{aligned} \partial \mathcal{P}_i / \partial t = & h_{i-1,i} \mathcal{P}_{i-1} - (h_{i,i-1} + h_{i,i+1}) \mathcal{P}_i \\ & + h_{i+1,i} \mathcal{P}_{i+1}, \end{aligned} \quad (8)$$

which is the discrete analog of (2) where the hopping rates are given by $h_{i,i+1} = h \exp(\Delta/2)$ and $h_{i+1,i} = h \exp(-\Delta/2)$ with $\Delta \equiv av_0/D_0$ and $h \equiv D_0/a^2$ [16].

Now let us introduce frozen disorder in the form of reversed sawteeth as in Fig. 1. Within the effective

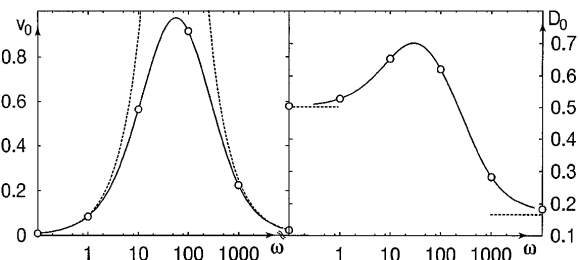


FIG. 2. The effective drift velocity v_0 and the effective diffusion coefficient D_0 as a function of the transition rate ω . The solid lines and the circles are obtained from the iterative procedure and from direct integration of (1), respectively. The broken lines represent the asymptotic behavior for small and for large ω . The length and time scales are given in units of the potential period a and the time scale $t_{sc} = fa^2/T$, respectively.

hopping model as given by (8), such a defect corresponds to an interchange of the corresponding hopping rates. Thus, one now has *random* hopping rates

$$h_{i,i+1} = he^{s_i\Delta/2} \quad \text{and} \quad h_{i+1,i} = he^{-s_i\Delta/2}, \quad (9)$$

where the random variable s_i has the values $s_i = 1$ and $s_i = -1$ for a normal and a reversed sawtooth, respectively.

For intermediate frequencies $\omega \approx \omega_1$, one jump in the effective hopping model represents the combination of one upwards transition and one downwards transition in order to overcome the nearest potential barrier and of the order of $t_{sc}/t_1 \approx (a/a_1)^2$ transitions as the particle slides down towards the minimum beyond this barrier. For large and for small ω , on the other hand, the relation between the effective hopping model and the original two-state model is somewhat different: (i) For *large* ω , the particle in the two-state model undergoes many transitions between its ground state and its excited state before it can diffuse beyond the nearest potential barrier. In the hopping model, this is described by a single jump with an appropriate hopping rate, and (ii) for *small* ω , the particle in its excited state can diffuse beyond several potential barriers before it falls back to its ground state. These events are likely to occur if the diffusion time exceeds $t_2 \equiv [(a_1 + a)/a_1]^2 t_1$, i.e., for $\omega \lesssim \omega_2 \equiv [a_1/(a_1 + a)]^2 \omega_1$. In the hopping model, such an event is described by several subsequent jumps in the same direction. Therefore, for $\omega \lesssim \omega_2$, the particle can overcome a reversed sawtooth in the two-state model just because it stays in the excited state for a sufficiently long time whereas it will always encounter the reversed sawtooth in the hopping model. This indicates that the latter model leads to an *overestimate* of the influence of the reversed sawtooth for small $\omega \lesssim \omega_2$. We will show, however, that this influence becomes small for small ω even within the hopping model. Therefore, the same behavior should apply, at least qualitatively, to the two-state model as well.

It is instructive to study the model as defined by (8) and (9) in the dilute limit of a single defect which consists of a certain number of reversed sawteeth [14]. One then finds that the particle is trapped in front of the defect for a certain waiting time τ until it is able to overcome the barrier arising from the defect.

For a finite defect concentration, the frozen disorder leads to a waiting time distribution $P(\tau)$ which exhibits a power law behavior for large τ . This can be understood from the following scaling argument as reviewed in [17]. If q is the probability to find a reversed sawtooth, the probability $P(N)$ to encounter a defect consisting of N such sawteeth is given by q^N . The waiting time τ_N , on the other hand, is expected to scale as $\tau_N \sim \exp(N\Delta)$. It then follows from $P(\tau)d\tau = P(N)dN$ that $P(\tau) \sim \tau^{-(1+\mu_0)}$ with $\mu_0 = \ln(1/q)/\Delta$. The latter value for the decay exponent μ is correct in the limit of small q since

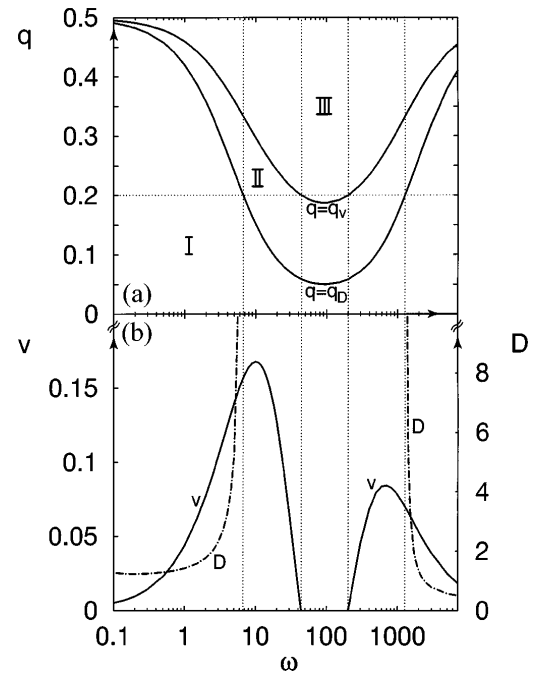


FIG. 3. (a) Phase diagram for driven ratchet with frozen disorder as a function of the transition rate ω and the defect concentration q , and (b) reentrant behavior for the effective drift velocity v (full lines) and the effective diffusion coefficient D (dot-dashed lines) as a function of the transition rate ω for fixed $q = \frac{1}{5}$. The numerical values on the left and on the right vertical axis correspond to v and D , respectively. The units are as in Fig. 2.

exact results for random hopping models [18,19] imply $P(\tau) \sim \tau^{-(1+\mu)}$ with $\mu = \ln(q^{-1} - 1)/\Delta$.

As long as the waiting time distribution $P(\tau)$ decays sufficiently fast, the moments $\langle \tau^n \rangle$ are finite for small n . Indeed, for $P(\tau) \sim \tau^{-(1+\mu)}$, the mean waiting time $\langle \tau \rangle$ is finite for the decay exponent $\mu > 1$ and the second moment $\langle \tau^2 \rangle$ is finite for $\mu > 2$. This already indicates that one has anomalous diffusion for $\mu < 2$ and anomalous drift for $\mu < 1$ as confirmed by more detailed calculations [17,19].

In the present context, the two phase boundaries $\mu = 2$ and $\mu = 1$ correspond to the critical defect concentrations $q = q_D$ and $q = q_v$, respectively, which are given by $q_D \equiv 1/[\exp(2\Delta) + 1]$ and $q_v \equiv 1/[\exp(\Delta) + 1]$ with $\Delta = av_0/D_0$ as before. The ω dependence of v_0 and D_0 , compare Fig. 2, now leads to ω dependent phase boundaries which separate three different scaling regimes (I), (II), and (III) of the driven ratchet with disorder as shown in Fig. 3(a). The transport behavior in these three regimes can be deduced from known results [19] for random hopping models.

In regime (I) with $0 < q < q_D$, both the effective drift velocity $v(q)$ and the effective diffusion coefficient $D(q)$ are finite. As q is increased, $v(q)$ decreases while $D(q)$ increases monotonically. The latter parameter diverges as $D(q) \sim 1/|q - q_D|$ as $q = q_D$ is approached from

below. In regime (II), the width of the distribution grows as $\sim t^{2/\mu}$ with $1 < \mu = \ln(q^{-1} - 1)/\Delta < 2$, i.e., faster than $t^{1/2}$ with time t but the drift is still characterized by a finite drift velocity $v(q)$. In fact, for the hopping model discussed here, the drift velocity is given by

$$v(q) = v_0(q_v - q)/[q_v + q(1 - 2q_v)] \quad (10)$$

both in regime (I) and in regime (II). Thus, as $q = q_v$ is approached from below, the drift velocity vanishes as $v(q) \sim |q - q_v|$. In regime (III) with $q_v < q < \frac{1}{2}$, both the drift and the diffusion are anomalous. The mean position of the particle and the width of its probability distribution are expected to grow as t^μ with $\mu = \ln(q^{-1} - 1)/\Delta = \ln(q^{-1} - 1)/\ln(q_v^{-1} - 1) < 1$.

The behavior of the effective drift velocity v and the effective diffusion coefficient D obtained in this way is shown in Fig. 3(b) as a function of the transition rate $\omega = \omega_\uparrow = \omega_\downarrow$ for fixed defect concentration $q = \frac{1}{5}$. The transport is normal for both low and high transition rates but exhibits the anomalous scaling regimes (II) and (III) at intermediate rates. In fact, comparison with Fig. 2 shows that these anomalous regimes appear precisely in the resonance regime where the ratchet is most effective in the absence of disorder [20].

In summary, we have shown that driven ratchets are quite sensitive to frozen disorder. Even though we have focused on two-state models, analogous behavior is expected for all single-particle ratchets. If some biophysical transport process is indeed based on such ratchets, the corresponding tracks have to be highly regular and the defect concentration q must be sufficiently small in order for the ratchets to operate in an efficient way. On the other hand, it would be most interesting to experimentally study the effects of frozen disorder in such systems since this will provide a nontrivial check on the underlying transport mechanism. Such disorder will also affect the behavior of ratchets containing large groups of interacting particles but this remains to be studied.

[1] A.F. Huxley, *Biophys. Chem.* **7**, 257 (1957).

[2] R. Feynman, R. Leighton, and M. Sands, *The Feynman Lectures on Physics* (Addison-Wesley, Reading, MA, 1965), Vol. I; R.D. Vale and F. Oosawa, *Adv. Biophys.* **26**, 97 (1990).

[3] See, e.g., J. A. Spudich, *Nature (London)* **348**, 284 (1990);

K. Svoboda, C. Schmidt, B. Schnapp, and S. Block, *Nature (London)* **365**, 721 (1993).

[4] N.J. Cordova, B. Ermentrout, and G.F. Oster, *Proc. Natl. Acad. Sci. U.S.A.* **89**, 339 (1992).

[5] S. Leibler and D.A. Huse, *J. Cell Biol.* **121**, 1357 (1993).

[6] M. Magnasco, *Phys. Rev. Lett.* **71**, 1477 (1993).

[7] R. Astumian and M. Bier, *Phys. Rev. Lett.* **72**, 1766 (1994).

[8] J. Prost, J.-F. Chauwin, L. Peliti, and A. Ajdari, *Phys. Rev. Lett.* **72**, 2652 (1994).

[9] F. Jülicher and J. Prost, *Phys. Rev. Lett.* **75**, 2618 (1995).

[10] C. Peskin, G. Odell, and G. Oster, *Biophys. J.* **65**, 316 (1993); W. Sung and P. Park, *Phys. Rev. Lett.* **77**, 783 (1996).

[11] J. Rousselet, L. Salome, A. Ajdari, and J. Prost, *Nature (London)* **370**, 446 (1994).

[12] L. Faucheux, L. Bourdieu, P. Kaplan, and A. Libchaber, *Phys. Rev. Lett.* **74**, 1504 (1995).

[13] See, e.g., H. Risken, *The Fokker-Planck Equation: Methods Of Solution And Applications* (Springer-Verlag, Berlin, 1989).

[14] In the present paper we give a brief summary of our results. The derivation of these results is somewhat lengthy and will be described elsewhere.

[15] For small and for large ω , the effective drift velocity behaves as $v_0 \sim \omega$ and $v_0 \sim 1/\omega$, respectively. The effective diffusion coefficient, on the other hand, attains the constant value $D_0 \approx (T/2f)\{1 + [u/\sinh(u)]^2\}$ for small ω and $D_0 \approx (T/f)[u/2\sinh(u/2)]^2$ for large ω with $u \equiv U_*/2T$.

[16] In the effective hopping model, the drift velocity and the diffusion coefficient are given by $2ah \sinh(\Delta/2)$ and $a^2h \cosh(\Delta/2)$, respectively, which approach v_0 and D_0 in the continuum limit of small a .

[17] J.-P. Bouchaud and A. Georges, *Phys. Rep.* **195**, 127 (1990).

[18] H. Kesten, M. Kozlov, and F. Spitzer, *Compositio Mathematica* **30**, 145 (1975).

[19] B. Derrida, *J. Stat. Phys.* **31**, 433 (1983); D. Aslangul, N. Pottier, and D. Saint-James, *J. Phys. (France)* **50**, 899 (1989).

[20] Numerical simulations of the original two-state model for defect concentrations $q = 0.05$ and $q = 0.27$ are in complete agreement with the theoretical predictions obtained here. For $q = 0.27$, the drift velocity $v(q)$ attains a finite value for $\omega = 1$ and $\omega = 10$ but decays to zero for $\omega = 100$ as one concludes from a finite size scaling analysis. The asymptotic values of $v(q)$ are in fair agreement with the values as given by (10).